Plant Archives Vol. 24, No. 1, 2024 pp. 1617-1627 e-ISSN:2581-6063 (online), ISSN:0972-5210

Plant Archives

Journal homepage: http://www.plantarchives.org

DOI Url : https://doi.org/10.51470/PLANTARCHIVES.2024.v24.no.1.226

REMOVAL OF CONGO RED DYE USING *ENTODON PROREPENS* (MITT.) JAEG. (A MOSS) BIOMASS: KINETICS, ISOTHERMS AND THERMODYNAMICS STUDY

Swati Secrain, Hiteshi Sabharwal, Neha Dogra, Anshul Pannu, Megha Sethi, Shefali Sharma and Sunita Kapila*

Bryology Lab, Department of Botany, Panjab University, Chandigarh - 160 014, India.

*Corresponding author E-mail : sunitakapilapu@gmail.com

(Date of Receiving-06-01-2024; Date of Acceptance-09-03-2024)

ABSTRACT

Congo Red, renowned for its chemical composition, characterized by two azo bonds (-N=N-). Congo Red not only highly toxic, but also resistant to degradation, contributing to its environmental persistence. This research was to analyze the efficiency of *Entodon prorepens* moss biomass for the removal of Congo Red dye from aqueous solutions. The impact of varying dye concentrations, contact time, pH, biomass dosage, and temperature was examined. FE-SEM and FTIR techniques were used in this research. Point-zero charge, kinetics, isotherms, and thermodynamics were investigated. The pseudo-second-order kinetic model provided the best fit to the data for CR removal. The Freundlich isotherm model provided an excellent fit with a maximum adsorption capacity of 118.45 mg/g. Adsorption was found to be endothermic and spontaneous. Microtoxicity assessment revealed that dye solutions after adsorption were less toxic than crude dye solutions. The biomass effectively removed CR and could be reused for up to three cycles.

Key words : Congo red, Adsorption, *Entodon prorepens*, Bryophyte, Moss, Biomass.

Introduction

Environmental pollution is eventually caused by dye-containing effluents from the textile, plastics, cosmetics, paper and tanning industries that is discharged into water bodies. Dyes that are extremely harmful to aquatic flora and fauna are gradually contaminating the water supply (Ramya and Sivasubramanian, 2020). Every year, up to 108 tonnes of various dyes are manufactured worldwide; azo dyes account for between 60 and 70 percent of this amount. Azo dyes are resistant to natural deterioration due to the presence of aromatic structures. Congo Red (diazo dye), which contains an aromatic amine in its formula, is recognized as a carcinogen (Harja *et al.*, 2022). It is used in histology staining, paper printing and cotton dyeing (Ramamoorthy *et al.*, 2016: Jabar *et al.*, 2020: Iqbal *et al.*, 2021). The fertility of the cladoceran *Ceriodaphnia dubia* is affected by a trace amount of Congo Red dye (Hermandez *et al.*, 2016). Prior to being released from industries into water resources, such pollutants must be optimized. Adsorption (Nodehi *et al.*, 2020; Adam *et al.*, 2021) ion exchange (Kim *et al.*, 2020), precipitation (Chowdhury and Bhowmik, 2021), photocatalysis (Zada *et al.*, 2020), electrochemical oxidation (Jin *et al.*, 2020) and other techniques have been proposed to remove dye particles from water. Adsorption, however, is considered very favorable due to the number of adsorbents, simplicity due to a low energy need, and low cost-effective technology.

Dye molecules from the wastewater are transferred onto a solid phase during the bio-sorption/adsorption process, which can then be recycled for additional usage (Yagub *et al.*, 2014). Adsorption is impacted by a number of variables, including the pH of the medium, dye and biosorbent/adsorbent concentrations, temperature, shaking rate, and the sort of functional groups that are present at the surface. These variables must be optimized

for the system to function well (Mishra and Maiti *et al*., 2020).

Mosses are cryptogamic plants, they can take in and hold onto nutrients, toxins, and moisture directly from the surrounding air. Their high surface-to-volume ratio, the simplicity of their anatomical structure, the lack of a cuticle, capacity to withstand harsh climatic conditions and great regenerative potential make them a vital tool for the monitoring of environmental pollution (Szczepaniak and Biziuk, 2003).

The cell wall surface of mosses consists of polyphenols, carboxyl, phosphoryl, and amine groups, as well as phosphodiesters which are frequently responsible for the high binding capabilities of mosses.The increased binding affinity to pollutants is explained by larger concentrations of uronic acids and mannuronic acids in the cell walls of mosses and liverworts, respectively, compared to cellulose and hemicellulose (Tipping *et al*., 2008).

The use of various adsorbents to remove the CongoRed (CR) dye from wastewater is currently the subject of active research. *Entodon* is a genus of mosses in the family Entodontaceae. In the present work, *Entodon prorepens* moss biomass has been used for efficient adsorptive removal of Congo Red dye, along with its kinetics, isotherms and thermodynamic models are studied. To assess the toxicity of dye, the microtoxicity test has been done on two bacteria *Bacillus subtilis* and *Escherichia coli*.

Materials and Methods

Preparation of chemicals and solvents

Congo Red (CR; Sigma-Aldrich, CAS: 573-58-0, $C_{32}H_{22}N_6Na_2O_6S_2$, 696.66 g/mol, PubChem CID 11313) is an anionic dye and is used as an adsorbate. Throughout the whole study, dye solutions were prepared using distilled water. 1gm of the dye powder was dissolved in 1L of distilled water in the volumetric flask to create the stock solution, which contained 1000 ppm of CR dye. By diluting dye solution with distilled water, the necessary dye concentrations were prepared. The pH of the solution was adjusted to the required pH value using 0.1 M of NaOH and 0.1 M of HCl.

Collection of plant material

Large quantity of the moss *Entodon prorepens* (Mitt.) Jaeg. (Fig. 1a) was collected from Mcleodganj Dharamshala in Kangra district, Himachal Pradesh, India (On the walls of the Army Cantt. area). The plants were thoroughly washed with distilled water to remove dust and unwanted particles from it. The washed biomass was dried at 60^{O}C for 48 hrs, ground and sieved with mesh #40 for ~400 micron average size particle and stored in an airtight container.

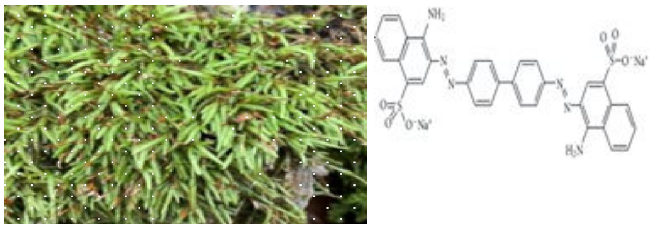

Fig. 1 : a) *Entodon prorepens* moss, **b)** Molecular structure of Congo Red dye.

Characterization using FE-SEM and FTIR technique

The surface morphology of moss biomass was examined using a field emission scanning electron microscope running at an accelerated voltage of 30 kV.Fourier Transform Infrared spectroscopy (FTIR) investigation of the dye solutions and the moss biomass before and after adsorption were conducted and interpreted at wavelengths in the range of 500- 4000 cm^{-1} (Perkin Elmer Spectrum, RX1, Germany).

Dye removal experiments

In order to optimise the various parameters affecting the dye removal experiments, batch mode tests were conducted. In 250 ml Erlenmeyer flasks with 100 ml test dye solution were shaken for 1-5 days at room temperature with a rotatory shaker at neutral pH. One factor was used at a time in the experiment keeping others factors constant. Experiments were carried out at different dye concentrations (25-100 ppm), biomass dosages (0.25gm-1gm), reaction times (1–5 days), temperatures (10–40°C) and pH (2–10) to optimize the variables that contribute for optimal adsorption efficiency. All the samples were filtered using Whatmann's filter paper No. 1 and once the filtrate had been collected, it was centrifuged at 10,000 rpm for 20 minutes. A UV-Visible Spectrophotometer EVOLUTION 201 was used to measure the dye content in the filtrate or final solution. The dye's maximum absorbance (λ_{max}=497nm) was used to record the absorbance results. Q_e was used to calculate the dye's maximal absorption.

$$Q_e = \frac{(C_o - C_e)V}{m} \quad (1)$$

Where, C_o and C_e are the initial and equilibrium concentration of dye (mgL^{-1}) respectively and V is the volume of dye in litres and m is the amount of biomass used in grams.

The percent removal of the dye solution was calculated by the following equation:

$$\%\ removal = \frac{C_o - C_e}{C_o} \times 100 \quad (2)$$

The mean values of C_e and Q_e were calculated after adsorption tests were performed in triplicate.

Desorption from moss biomass

The dye-loaded adsorbent biomass was recycled by using acid, base, and double distilled water. The dye-loaded adsorbent was treated with 0.1M HCl, 0.1M NaOH and double distilled water. The dye particles were desorbed and biomass was used for further adsorption experiments (Zhou *et al*., 2019).

Point of Zero charge (pHpzc)

The point of zero charge's (pHpzc) is defined as the solution's pH at which the adsorbent's surface charge is zero. In this, the initial pH values (pH_i) of Congo Red dye solutions (50 ppm) were adjusted in the range of 2-10 using NaOH and HCl solutions. 1 gm of biomass dose was added and all experiments were performed in triplicate. The final pH values (ΔpH) were recorded after shaking the solutions for 24 hrs at 120 rpm.

Adsorption kinetics

The pseudo-first-order, pseudo-second-order, and intra-particle diffusion models were utilized to analyze the experimental data to assess the adsorption process's kinetic mechanism (Aysu and Kucuk, 2015). Equation (3) defines the pseudo-first-order model's linear form.

$$\ln(q_e - q_t) = \ln q_e - K_1 \quad (3)$$

Here, q_t (mg/g) and q_e (mg/g) are the adsorption capacities at time t (min) and the equilibrium condition, and k_1 (min^{-1}) is the pseudo-first-order Lagergren rate constant, respectively. The adsorption kinetic was assessed using the following pseudo-second-order model:

$$\frac{t}{q_t} = \frac{1}{k_2 q_e^2} + \frac{t}{q_e} \quad (4)$$

Where, k_2 (g/mg min) is the pseudo-second-order model's rate constant. Most likely, dye particles were transported from the bulk to the solid phase through intra-particle diffusion. The intra-particle diffusion models is:

$$q_t = k_{id} t^{\frac{1}{2}} + C \quad (5)$$

Where, C and k_{id} are constants for the intra-particle diffusion rate constant (mg/g $min^{1/2}$) and the boundary layer thickness constant (mg/g), respectively.

Adsorption isotherm

Langmuir isotherm, Freundlich isotherm and Temkin isotherm models were used to estimate the adsorption equilibrium (Saeed *et al*., 2010: Sepehr *et al*., 2014). Langmuir isotherm is based on the premise that there are a finite number of identical adsorption sites in a monolayer and that the surface energy distribution is homogenous. Langmuir isotherm is shown in linear form in Equation (6).

$$\frac{1}{q_e} = \frac{1}{q_m} + \frac{1}{K_L q_m C_e} \quad (6)$$

Where, C_e is the equilibrium concentration of adsorbate (mg/L), q_e is the equilibrium amount of adsorbate per one gram of the sorbent (mg/g), q_m is maximum adsorption capacity (mg/g) and K_L is Langmuir constant (L/mg).

The Freundlich isotherm model for an adsorption heterogeneous surface is typically described by the following equation.

$$\ln q_e = \ln K_F + \frac{1}{n} \ln C_e \quad (7)$$

Freundlich constants are K_F (((mg/g)/(mg/L)$^{-1}$/n)) and n.

Temkin isotherm also applies to heterogeneous adsorption and analyses the interactions between an adsorbent and an adsorbate on a surface. Eq. (8) provides the model's linear form

$$q_e = \frac{RT}{b_T} \ln K_T + \frac{RT}{b_T} \ln C_e \quad (8)$$

Where, respectively, T, R, b_T and K_T stand for the equilibrium binding constant (L/g), the enthalpy of adsorption (J/mol), Temkin constant (K), the absolute temperature (K), the gas universal constant (8.314 J/mol K).

Average relative error (ARE) and nonlinear chi-square test (χ^2) were performed for error and precise analysis of the above models (Foo and Hameed, 2010).

$$ARE = \sum_{i=1}^{n} \left| \frac{(q_{e,\exp} - q_{e,cal})}{q_{e,cal}} \right| \quad (9)$$

$$\chi^2 = \sum_{i=1}^{n} \left| \frac{(q_{e,\exp} - q_{e,cal})^2}{q_{e,cal}} \right| \quad (10)$$

Thermodynamic studies

For CR adsorption onto the moss biomass, the standard Gibbs free energy ΔG° (J/mol) change was assessed. The following formulae were used to determine this parameter:

$$K_c = \frac{Q_e}{C_e} \quad (11)$$

$$\Delta G = -RT \ln K_c \quad (12)$$

Therefore, the entropy difference, ΔS° (J/mol K) and the enthalpy change, ΔH° (J/mol) were calculated using Eq. (13).

$$\ln K_c = \frac{\Delta S^0}{R} - \frac{\Delta H^0}{RT} \quad (13)$$

Microtoxicity assessment

The toxicity of the untreated and treated CR solutions by *Entodon prorepens* biomass was assessed using the *Bacillus subtilis* MTCC 441 and *Escherichia coli* MTCC 585 bacteria (Asses *et al.*, 2018). The growth of two bacterial strains was examined with 200 mg L^{-1} of CR solution, added crude and after adsorption. Ciprofloxacin (antibiotic) was taken as positive control and distilled water as negative control. *E. coli* and *B. subtilis* had an incubation temperature of 37°C and 30°C, respectively.

Results and Discussion

Characterization using FE-SEM and FTIR techniques

FE-SEM analysis : The surface characteristics of moss powder before and after CR adsorption were obtained by FE-SEM images as shown in Fig. 2 (a-b).

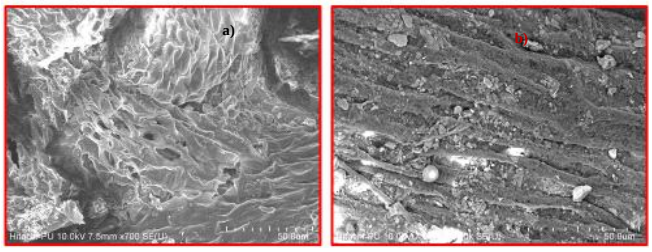

Fig. 2 : SEM micrographs **a)** Before treatment, **b)** After treatment.

The images before and after CR adsorption reveal that *Entodon* moss has porous, irregular and cellular texture, and the dye particles adsorb over its surface.

FTIR analysis : FTIR spectra of Congo Red dye before and after treatment with moss biomass has been recorded (Fig. 3 (a-b)).

The FTIR evaluation of the biomass was performed both before and after treatment in CR solution in order to understand the nature of the functional groups accountable for the adsorption (Fig. 4 (a-b)).

Dye removal experiments

Optimization of parameters

The UV-Vis spectra of the dye solution before and after treatment with biomass of *Entodon prorepens* were recorded from 400nm to 600nm (Fig. 5). Congo Red dye showed maximum absorbance at 497 nm. However, there was a remarkable decrease in absorbance peaks after the treatment with moss biomass. The area under the absorption band was used to monitor the percentage of dye.

Effect of initial dye concentration and contact time : The impact of the initial dye concentration (25 ppm, 50 ppm, 75 ppm, 100 ppm) was noted with 1gm of biomass and it was found that the maximum adsorption was observed at 50 ppm with 93.3% removal (Fig. 6). It can be interpreted that the transfer of dye molecules from bulk solution to biomass surface can be understood as an increase in the density gradient between the aqueous and solid phases with an increase in dyeconcentration (Bentahar *et al.*, 2018). The adsorption of dye solution on biomass increases with increase in time duration and after that equilibrium was attained. The high removal rate at the beginning of the contact period was caused by the broad surface area that was initially available for the dye to adsorb, and with time, the capacity of the adsorbent steadily depleted because of the blockage of active dye binding sites (Wanyonyi *et al.*, 2014).

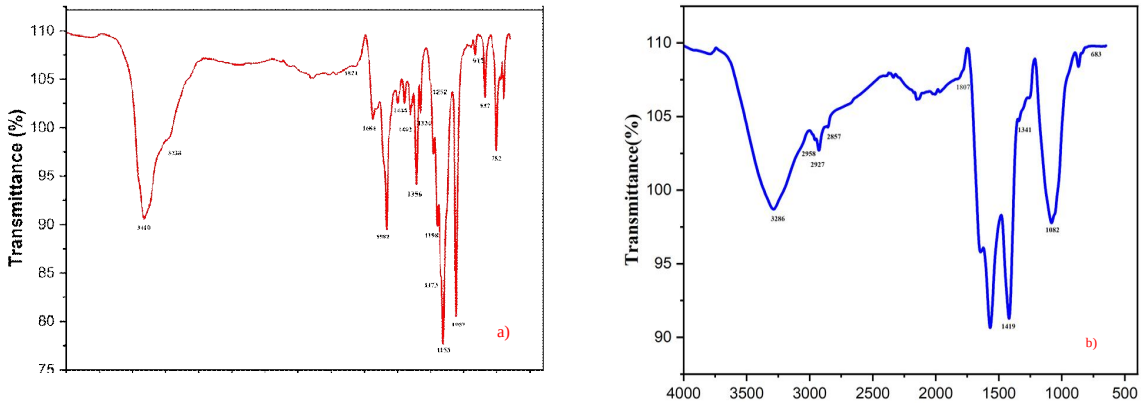

Fig. 3 : FTIR spectra of Congo Red dye **a)** Before adsorption, **b)** After adsorption.

Table 1 : Functional groups present in dye solutions and moss biomass (powder) before and after adsorption according to FTIR data.

	CR (Before)		**CR (After)**		**Moss biomass (Before)**		**Moss biomass (After)**
Wave number (cm^{-1})	**Functional groups**	**Wave number (cm^{-1})**	**Functional groups**	**Wave number (cm^{-1})**	**Functional groups**	**Wave number (cm^{-1})**	**Functional groups**
3410	-O-H stretch	3286	-OH stretch/ alkyene	3413	-OH stretch	2923	OH/-NH stretch
3238	-O-H stretch/ -COOH stretching	2958	-OH stretch/ -NH stretch	3011	-CH/-OH/- COOH stretch	1821	-CH bend
1821	-C=C=C- stretch/alkene, -CH- bend/ aromatic compound	2927	-OH stretch/ -NH stretch	2926	-CH/-NH/-OH stretch	1684	-CN/-C=O stretch
1684	–C-H- bend	2857	-NH stretch	2855	-NH/-CH stretch	1444	-NH/-C=C- bend
1582	alkenyl -C=C- stretch/-C=N stretch-	1807	-N=N-/CH bend/ -C=O stretch	2033	-N=C=S- stretch	1356	-OH/ -S=O stretch
1446	-NH bend amine/ aromatic -CH plane bend/-C=C stretch / cyclic alkene	1419	-OH bend	1744	-CH/-C=O/ester stretch		
1402	-C=C-C aromatic ring stretch	1341	-OH bend	1617	-C=C/-NH stretch		
1356	$-CH_3$ group	1082	-CF stretch/-CN stretch	1382	-S=O/-OH stretch		
1324	-O-H bend/-S=O stretch	683	-C-Br stretch	1317	-OH bend/ Phenol		
1198	-O-H bend/-C-F stretch/ strong –S=O- stretch/ -C-N stretch			1240	-C-N/-C-O stretch		
1173	-C-F stretch/-C-O stretch			1159	-C-N/-C-O stretch		
1153	-C-N stretch aromatic amine/ C-F stretch/-C-O stretch			1065	-C-O/-S=O stretch		

Effect of pH : The adsorption of dye particles was examined over a pH range of 2-10 and it was found to be maximum at pH 4 with 91% removal (Fig. 7). At pH 4.0, there is a considerable electrostatic attraction between the positively charged surface of the adsorbent and the anionic dye. The number of negatively charged sites grows while the number of positively charged sites decreases as the pH of the system rises. Furthermore, reduced CR adsorption at alkaline pH is caused by the presence of excess -OH ions competing for adsorption sites with the dye anions. Adsorption of CR on the waste orange peel (Hua *et al*., 2023) and activated carbon (Namasivayam and Kavitha, 2002) have been reported with similar findings.

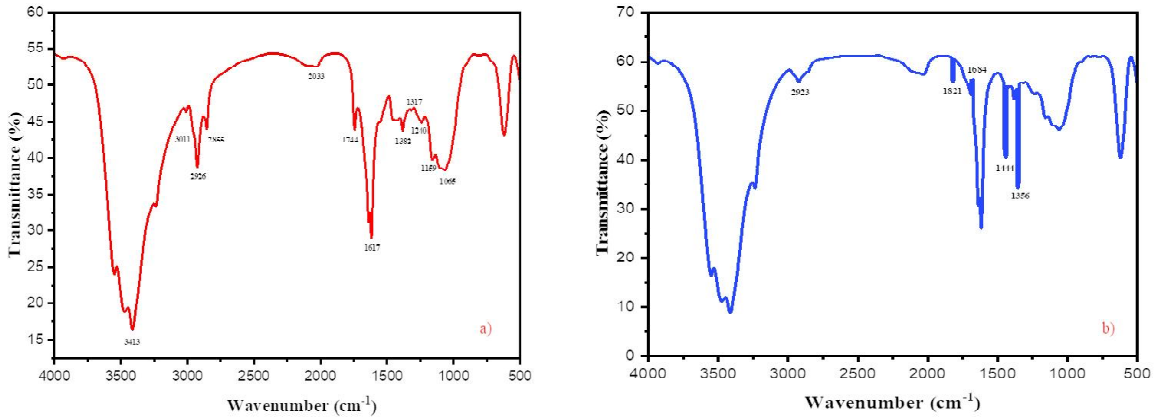

Fig. 4 : FTIR spectra of moss biomass **a)** Before adsorption, **b)** After adsorption.

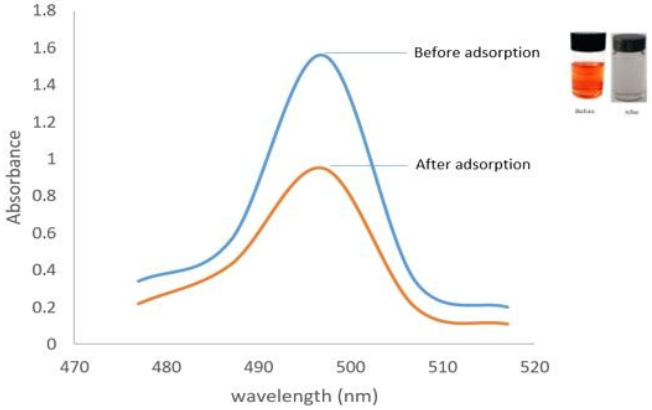

Fig. 5 : UV-Vis spectra of the dye solution before and after treatment.

adsorption due to the thermal deactivation of the dye-binding active sites on the surface of biomass. Greater adsorption value could also be caused by increased movement of dye ions with temperature. There is a chance that more molecules will acquire sufficient energy to engage with the surface's active site (Kaur *et al.*, 2013).

Desorption from moss biomass

The recycle and reuse process has been used but after a few cycles, adsorption efficiency dropped because the surface porosity of the adsorbent biomass collapsed, blocking pores and preventing dye molecules from adhering to the surface (Essekri *et al.*, 2021). The adsorbent was

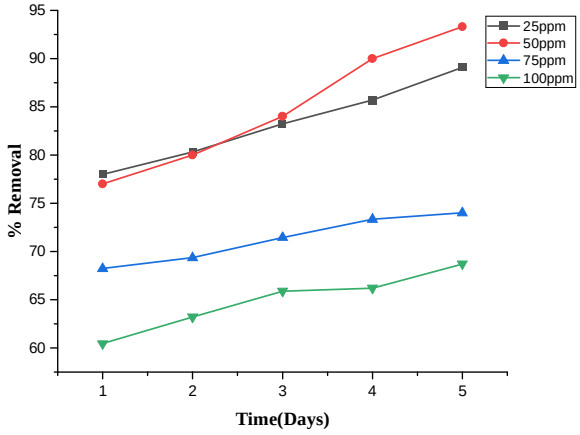

Fig. 6 : Effect of initial dye concentration.

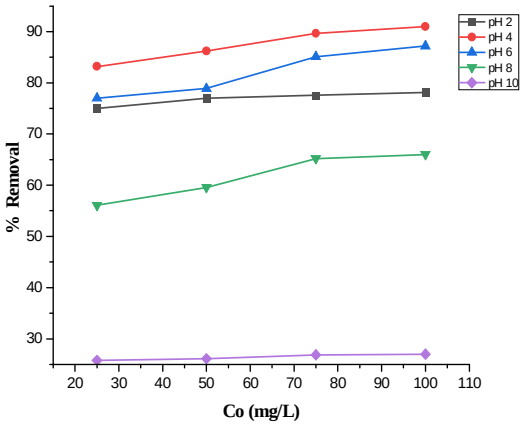

Fig. 7 : Effect of pH.

Effect of dosage : It was found that the adsorption percentage increases as the amount of biomass increases (Fig. 8). Because there is an increase in the number of active sites with an increase in biomass amount.

Effect of temperature : It was observed that maximum adsorption was recorded with an increase in temperature from 10°C to 30°C (Fig. 9). Hence, the process was observed to be endothermic in nature. After that, the temperature rises but there is a sudden fall in

recycled almost three times with base, with removal efficiencies of 78%, 65% and 50% for dyes. While with acid treatment, the ability of the adsorbent to adsorb the dye particles was reduced, with 35%, 26% and 18%. Due to pore blockage on the surface of the moss biomass, distilled water showed a very low capacity for adsorbent reusability with dye removal rates of 25%, 11% and 8% (Fig. 10).

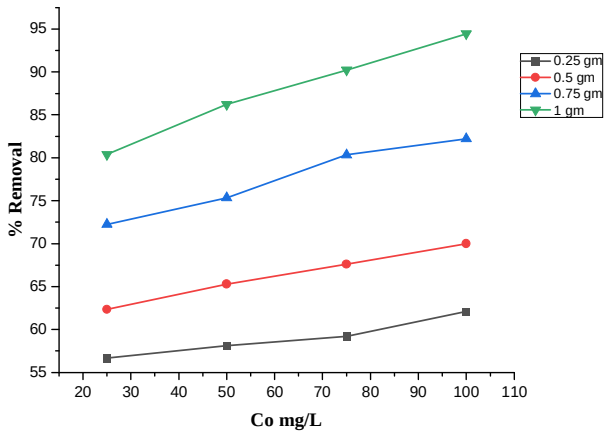

Fig. 8 : Effect of biomass dosage.

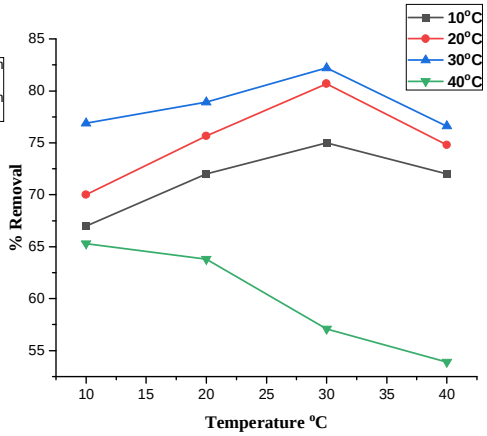

Fig. 9 : Effect of temperature.

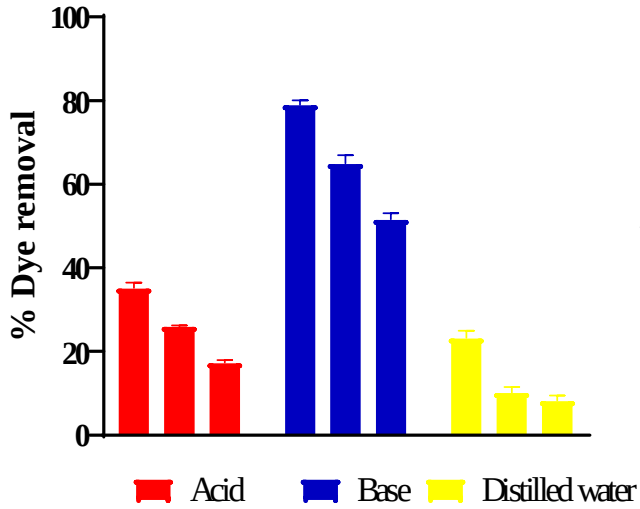

Fig. 10 : Recycling of adsorbent.

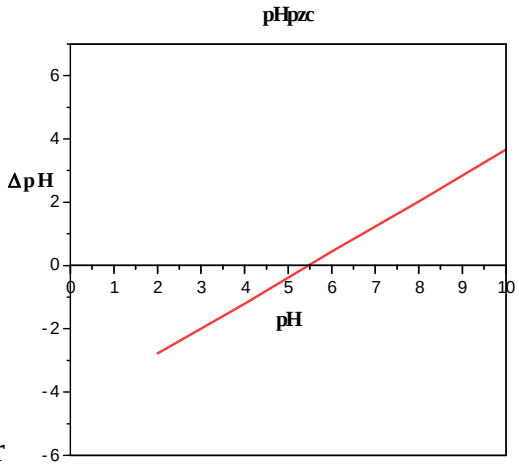

Fig 11: Point zero charge of Congo Red dye.

Point Zero charge

The presence of various functional groups, such as COO- and OH-, caused the adsorption of cationic dye to occur at pH >pHpzc. On the other hand, anionic dye adsorption took place at pH<pHpzc (Savova *et al.*, 2003). As indicated in Fig. 11, the pHpzc of the moss biomass powder used in this experiment was found to be 5.5. This means that the adsorbent surface carries a positive charge when the pH is below pHpzc and a negative charge when the pH is above pHpzc.Similar results have been observed for removal of CongoRed dye using natural raw material (Hachani *et al.*, 2017).

Adsorption kinetics

The results of evaluating the linear fitness of the $\log(q_e-q_t)$ data vs. t, t/q_t vs. t, and q_e vs. $t_{1/2}$ are shown in Fig. 12 in accordance with Eqs. (3) through (5). Table 2 data show that the correlation coefficient (R^2) derived from pseudo-second-order kinetic (0.997) for initial CR concentrations of 50 mg/L higher than that for pseudo-first-order (0.93) and intra-particle diffusion models (0.95), respectively. Results were better than those for intra-particle diffusion and pseudo-first-order kinetics models. Moreover, the estimated equilibrium adsorption capacity (q_e) and experimental adsorption capacity of the pseudo-second-order model are extremely correlated. It also demonstrates the relevance of the model with pseudo-second order to estimate the adsorption process regulated by chemisorption (Chen *et al.*, 2014; Islam *et al.*, 2015; Sriram *et al.*, 2020), where the adsorption mechanism can be described by electron exchange or sharing amongst both the adsorbent and adsorbate (Miao *et al.*, 2021). It implies that either two molecules were adsorbed on a single site or that one molecule interacts with two adsorption sites.

Adsorption isotherms

With the help of the Langmuir isotherm, Freundlich isotherm, and Temkin isotherm models, the adsorption parameters were assessed. Table 3 lists calculated constants related to these models. The Langmuir model's R^2 value is greater than those of the other linear coefficients, as the data in Table 3. The ARE and S«^{2} values calculated using the Langmuir isotherm are also

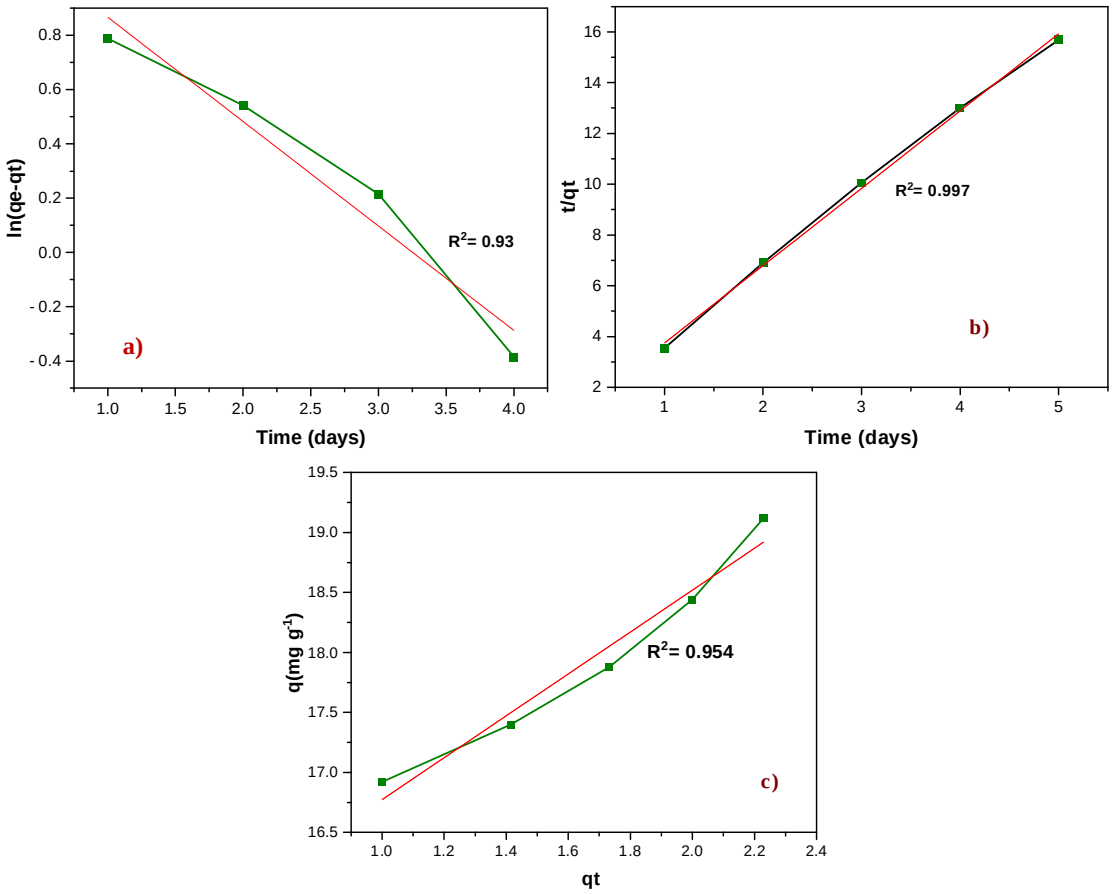

Fig. 12 : Adsorption kinetics of CR adsorbed by moss biomass: **(a)** pseudo-first-order model, **(b)** pseudo-second-order model, **(c)** intra-particle diffusion model.

Table 2 : Adsorption kinetic parameters for adsorption of Congo Red on to the moss biomass.

	q_e	K_1	R^2
Pseudo 1st order rxn	17.852	1.780	0.935
	q_e	K_2	R^2
Pseudo 2nd order rxn	19.72	3.611	0.997
	q_e	K_{id}	R^2
3rd oder rxn	19.95	0.224	0.954

lower than comparable parameters associated with the Freundlich isotherm and Temkin isotherm. It suggests that compared to the Freundlich as well as Temkin models, the Langmuir model is better able to reflect the results that were observed. The maximal adsorption capacity of Congo Red was determined by Eq. (6) to be 118.450 mg/g.

The adsorption of a monolayer onto a surface having a restricted amount of identical sites, where each site is energetically equal, is the foundation of the Langmuir isotherm model. Adsorbed molecules do not interact and are equal. The Langmuir isotherm, which suggests that the surface of the adsorbent utilized in the removal of

Table 3 : Adsorption isotherm models (constants and error analysis).

	Langmuir isotherm		**Freundlich isotherm**		**Temkin isotherm**
R^2	0.98	R^2	0.95	R^2	0.93
q_{max}	118.450	1/n	0.525	b_T	0.575
K_L	1.737	K_f	6.088	K_T	433.3
ARE	0.011	ARE	0.63	ARE	1.33
χ^2	0.002	χ^2	7.41	χ^2	8.33

Congo Red is homogeneous, best fits the experimental results (Ma and Wang, 2015; Karimaian *et al.*, 2013).

Thermodynamic studies

To determine the values of enthalpy change, ΔH^0, and entropy change, ΔS^0, ln K_c were plotted against 1/T (Fig. 13). The value of $\Delta G°$ was evaluated using Eq. (11). Table 4 provides the values of the thermodynamic parameters. The endothermic nature of the adsorption process is indicated by the positive value of $\Delta H°$. While the value of $\Delta S°$ decreases with an increase in temperature indicates that the rise in temperature decreases the randomness in the system. The $\Delta G°$

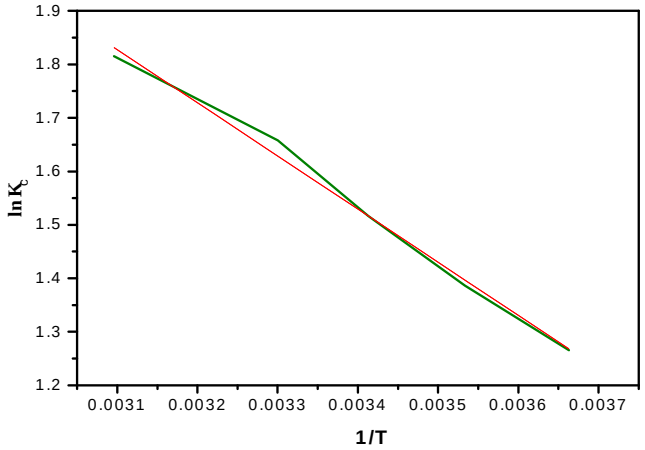

Fig. 13 : ln K_c vs. 1/T plot.

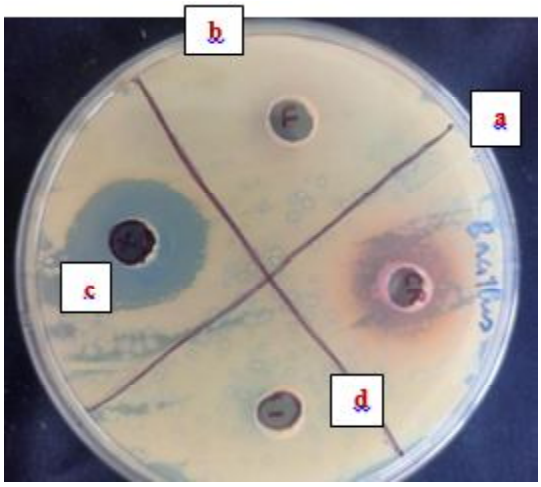

Fig. 14 : *Bacillus subtilis* **a).** CR, **b).** treated CR, **c).** + control, **d).** –ve control.

negative value discovered in this study suggests that the system is feasible in nature. As the temperature rises, the negative value of ΔG° value increases. The conclusion suggests that the spontaneity of the adsorption process is directly related to the system temperature.

Microtoxicity assay

Using *Bacillus subtilis* MTCC 441 and *Escherichia coli* MTCC 585 strain microbiological cultures, the toxicity of untreated and treated Congo Red has been assessed. In crude CongoRed (200 mgL^{-1}), the inhibition zones of *Bacillus subtilis* MTCC 441 and *Escherichia coli* MTCC 585 strains were 20 mm and 18 mm in diameter, as compared to positive control 25mm and 21mm, respectively (Figs. 14, 15). Whereas, media containing treated dye solution with adsorbent biomass showed an improvement in bacterial growth than crude dye solution. Therefore, the CR seem to get adsorb over the biomass surface after treatment.

Table 4 : Adsorption thermodynamic parameters for adsorption of CR onto the moss biomass.

Temp (K)	ΔG ($KJ\ mol^{-1}$)	ΔH ($KJ\ mol^{-1}$)	H-G	S=(H-G)/T ($JK^{-1}\ mol^{-1}$)
273	-0.3156		8.57955	0.031427
283	-0.3457		0.3457	0.001222
293	-0.3782	8.26395	0.3782	0.001291
303	-0.4135		0.4135	0.001365
323	-0.4527		0.4527	0.001402

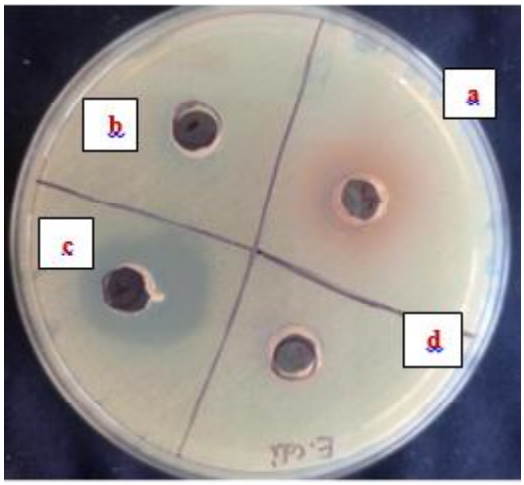

Fig. 15 : *Escherichia coli* **a).** CR, **b).** treated CR, **c).** + control, **d).** –ve control.

Conclusion

Entodon prorepens biomass was found to be efficient and inexpensive adsorbent for the removal of Congo Red dye. With a dye solution concentration of 50 ppm, the highest adsorption was seen with a rise in the amount of biomass of adsorbent. A combination of 30°C, and pH 4.0 was determined to be ideal. Up to three rounds of recycling and utilization of dye-loaded adsorbent by the base were possible, with 78%, 65% and 50%. The Langmuir isotherm model, as opposed to the Freundlich isotherm and Temkin isotherm models provided a more accurate description of the adsorption behaviour. The calculated maximal adsorption capacity was 118.45 mg/g as a result. The linear form of the pseudo-second-order rate model was used to fit the adsorption kinetics. Thermodynamic terms like ΔG, ΔH and ΔS were also assessed. The adsorption process is endothermic and spontaneous, respectively, as evidenced by the negative value of the ΔG° and the positive value of the ΔH°. As a result, biomass from *Entodon prorepens* can be utilized as a substitute adsorbent to treat wastewater that contains Congo Red dye.

Acknowledgment

The authors would like to thank the UGC funding agency and SAIF-CIL Instrumental Lab, Panjab University, Chandigarh.

References

Adam, A.M.A., Saad H.A., Atta A.A., Alsawat M., Hegab M.S., Refat M.S. and Younes A.A. (2021). Preparation and characterization of new $CrFeO_3$-carbon composite using environmentally friendly methods to remove organic dye pollutants from aqueous solutions. *Crystals*, **11(8)**, 960. https://doi.org/10.3390/cryst11080960.

Arellano-Cardenas, S., Lopez-Cortez S., Cornejo-Mazón M., and Mares-Gutierrez J.C. (2013). Study of malachite green adsorption by organically modified clay using a batch method. *Applied Surface Science*, **280**, 74-78.https://doi.org/10.1016/j.apsusc.2013.04.097.

Asses, N., Ayed L., Hkiri N. and Hamdi M. (2018). Congo red decolorization and detoxification by *Aspergillus niger*: removal mechanisms and dye degradation pathway. *BioMed Res. Int.*, *2018*. https://doi.org/10.1155/2018/3049686.

Aysu, T. and Kucuk M.M. (2015). Removal of crystal violet and methylene blue from aqueous solutions by activated carbon prepared from *Ferula orientalis*. *Int. J. Environ. Sci. Technol.*, **12**, 2273-2284. https://doi.org/10.1007/s13762-014-0623-y.

Bentahar, S., Dbik A., El Khomri M., El Messaoudi N. and Lacherai A. (2018). Removal of a cationic dye from aqueous solution by natural clay. *Groundwater for Sustainable Development*, **6**, 255-262. https://doi.org/10.1016/j.gsd.2018.02.002.

Chen, H., Yan T. and Jiang F. (2014). Adsorption of Cr (VI) from aqueous solution on mesoporous carbon nitride. *J. Taiwan Inst. Chem. Engs.*, **45(4)**, 1842-1849. https://doi.org/10.1016/j.jtice.2014.03.005.

Chowdhury, N.K. and Bhowmik B. (2021). Micro/nanostructured gas sensors: the physics behind the nanostructure growth, sensing and selectivity mechanisms. *Nanoscale Advances*, **3(1)**, 73-93. https://doi.org/10.1039/D0NA00552E.

Essekri, A., Hsini A., Naciri Y., Laabd M., Ajmal Z., El Ouardi M. and Albourine A. (2021). Novel citric acid-functionalized brown algae with a high removal efficiency of crystal violet dye from colored wastewaters: insights into equilibrium, adsorption mechanism and reusability. *Int. J. Phytoremed.*, **23(4)**, 336-346. https://doi.org/10.1080/15226514.2020.1813686.

Foo, K.Y. and Hameed B.H. (2010). Insights into the modelling of adsorption isotherm systems. *Chem. Engg J.*, **156(1)**, 2-10. https://doi.org/10.1016/j.cej.2009.09.013.

Hachani, R., Sabir H., Sana N., Zohra K.F. and Nesrine N.M. (2017). Performance Study of a Low cost Adsorbent—Raw Date Pits—for Removal of Azo Dye in Aqueous Solution: Rahima *et al. Water Environ. Res.*, **89(9)**, 827-839. https://doi.org/10.2175/106143017X14902968254863.

Harja, M., Buema G. and Bucur D. (2022). Recent advances in removal of Congo Red dye by adsorption using an industrial waste. *Scientific Reports*, **12(1)**, 6087. https://doi.org/10.1038/s41598-022-10093-3.

Hernandez-Zamora, M., Martinez-Jeronimo F., Cristiani-Urbina E. and Canizares-Villanueva R.O. (2016). Congo red dye affects survival and reproduction in the cladoceran *Ceriodaphnia dubia*. Effects of direct and dietary exposure. *Ecotoxicology*, **25**, 1832-1840. https://doi.org/10.1007/s10646-016-1731-x.

Hua, Z., Pan Y. and Hong Q. (2023). Adsorption of Congo red dye in water by orange peel biochar modified with CTAB. *RSC Advances*, **13(18)**, 12502-12508. https://doi.org/10.1039/D3RA01444D.

Islam, M.A., Benhouria A., Asif M. and Hameed B.H. (2015). Methylene blue adsorption on factory-rejected tea activated carbon prepared by conjunction of hydrothermal carbonization and sodium hydroxide activation processes. *J. Taiwan Inst. Chem. Engs.*, **52**, 57-64. https://doi.org/10.1016/j.jtice.2015.02.010.

Iqbal, J., Shah N.S., Sayed M., Niazi N.K., Imran M., Khan J.A. and Howari F. (2021). Nano-zerovalent manganese/biochar composite for the adsorptive and oxidative removal of Congo-red dye from aqueous solutions. *J. Hazard. Mat.*, **403**, 123854. https://doi.org/10.1016/j.jhazmat.2020.123854.

Jabar, J.M., Odusote Y.A., Alabi K.A. and Ahmed I.B. (2020). Kinetics and mechanisms of congo-red dye removal from aqueous solution using activated *Moringa oleifera* seed coat as adsorbent. *Appl. Water Sci.*, **10(6)**, 1-11. https://doi.org/10.1007/s13201-020- 01221-3.

Jin, J., Zhang Y., Li G., Chu Z. and Li G. (2020). Synthesis and enhanced gas sensing properties of iron titanate and copper titanate nanomaterials. *Materials Chemistry and Physics*, **249**, 123016. https://doi.org/10.1016/j.matchemphys.2020.123016.

Karimaian, K.A., Amrane A., Kazemian H., Panahi R. and Zarrabi M. (2013). Retention of phosphorous ions on natural and engineered waste pumice: Characterization, equilibrium, competing ions, regeneration, kinetic, equilibrium and thermodynamic study. *Applied Surface Science*, **284**, 419-431. https://doi.org/10.1016/j.apsusc.2013.07.114.

Kaur, S., Rani S. and Mahajan R.K. (2013). Adsorption kinetics for the removal of hazardous dye congo red by biowaste materials as adsorbents. *J. Chem.*, *2013*. https://doi.org/10.1155/2013/628582.

Kim, J.H., Park G.D. and Kang Y.C. (2020). Amorphous iron oxide–selenite composite microspheres with a yolk–shell structure as highly efficient anode materials for lithium-ion batteries. *Nanoscale*, **12(19)**, 10790-10798. https://doi.org/10.1039/D0NR01905D.

Ma, Q. and Wang L. (2015). Adsorption of Reactive blue 21 onto functionalized cellulose under ultrasonic pretreatment: Kinetic and equilibrium study. *J. Taiwan Inst. Chem. Engs.*, **50**, 229-235.https://doi.org/10.1016/

j.jtice.2014.12.018.

Miao, J., Zhao X., Zhang Y.X. and Liu Z.H. (2021). Feasible synthesis of hierarchical porous MgAl-borate LDHs functionalized Fe_3O_4@ SiO_2 magnetic microspheres with excellent adsorption performance toward congo red and Cr (VI) pollutants. *J. Alloys and Compounds*, **861**, 157974. https://doi.org/10.1016/j.jallcom.2020.157974.

Mishra, S. and Maiti A. (2020). Biological methodologies for treatment of textile wastewater. *Environmental Processes and Management: Tools and Practices*, 77-107. http://dx.doi.org/10.1007/978-3- 030-38152-3_6.

Namasivayam, C. and Kavitha D. (2002). Removal of Congo Red from water by adsorption onto activated carbon prepared from coir pith, an agricultural solid waste. *Dyes and Pigments*, **54(1)**, 47-58. https://doi.org/10.1016/S0143-7208(02)00025-6.

Nodehi, R., Shayesteh H. and Kelishami A.R. (2020). Enhanced adsorption of congo red using cationic surfactant functionalized zeolite particles. *Microchem. J.*, **153**, 104281.https://doi.org/10.1016/j.microc.2019.104281.

Ramamoorthy, A., Ravi S., Jeddy N., Thangavelu R. and Janardhanan S. (2016). Natural alternatives for chemicals used in histopathology lab-A literature review. *J. Clin. Diagn. Res.: JCDR*, **10(11)**, EE01. https://doi.org/10.7860/JCDR/2016/23420.8860.

Ramya Sankar, M.S. and Sivasubramanian V. (2020). Application of statistical design to optimize the electrocoagulation of synthetic Congo red dye solution and predicting the mechanism. *Int. J. Environ. Sci. Technol.*, **17**, 1373-1386. https://doi.org/10.1007/s13762-019-02555- 5.

Saeed, A., Sharif M. and Iqbal M. (2010). Application potential of grapefruit peel as dye sorbent: kinetics, equilibrium and mechanism of crystal violet adsorption. *J. Hazard. Mat.*, **179(1-3)**, 564-572. https://doi.org/10.1016/j.jhazmat.2010.03.041.

Savova, D., Petrov N., Yardim M.F., Ekinci E., Budinova T., Razvigorova M. and Minkova V. (2003). The influence of the texture and surface properties of carbon adsorbents obtained from biomass products on the adsorption of manganese ions from aqueous solution. *Carbon*, **41(10)**, 1897-1903. https://doi.org/10.1016/S0008- 6223(03)00179-9.

Sepehr, M.N., Amrane A., Karimaian K.A., Zarrabi M. and Ghaffari H.R. (2014). Potential of waste pumice and surface modified pumice for hexavalent chromium removal: characterization, equilibrium, thermodynamic and kinetic study. *J. Taiwan Inst. Chem. Enggs.*, **45(2)**, 635-647.https://doi.org/10.1016/j.jtice.2013.07.005.

Sriram, G., Uthappa U.T., Losic D., Kigga M., Jung H.Y. and Kurkuri M.D. (2020). Mg–Al-layered double hydroxide (LDH) modified diatoms for highly efficient removal of Congo red from aqueous solution. *Appl. Sci.*, **10(7)**, 2285. https://doi.org/10.3390/app10072285.

Szczepaniak, K. and Biziuk M. (2003). Aspects of the biomonitoring studies using mosses and lichens as indicators of metal pollution. *Environ. Res.*, **93(3)**, 221-230. https://doi.org/10.1016/s0013-9351(03)00141-5.

Tipping, E., Vincent C.D., Lawlor A.J. and Lofts S. (2008). Metal accumulation by stream bryophytes, related to chemical speciation. *Environ. Poll.*, **156(3)**, 936-943. https://doi.org/10.1016/j.envpol.2008.05.010.

Wanyonyi, W.C., Onyari J.M. and Shiundu P.M. (2014). Adsorption of Congo red dye from aqueous solutions using roots of *Eichhornia crassipes*: Kinetic and equilibrium studies. *Energy Procedia*, **50**, 862-869. https://doi.org/10.1016/j.egypro.2014.06.105.

Yagub, M.T., Sen T.K., Afroze S. and Ang H.M. (2014). Dye and its removal from aqueous solution by adsorption: A review. *Advances in Colloid and Interface Science*, **209**, 172-184.https://doi.org/10.1016/j.cis.2014.04.002.

Zada, A., Muhammad P., Ahmad W., Hussain Z., Ali S., Khan M. and Maqbool M. (2020). Surface plasmonic assisted photocatalysis and optoelectronic devices with noble metal nanocrystals: Design, synthesis and applications. *Advanced Functional Materials*, **30(7)**, 1906744. https://doi.org/10.1002/adfm.201906744.

Zhou, Y., Lu J., Zhou Y. and Liu Y. (2019). Recent advances for dyes removal using novel adsorbents: A review. *Environ. Poll.*, **252**, 352-365. https://doi.org/10.1016/j.envpol.2019.05.072.

Abbreviation: CR (Congo Red)